ELSEVIER

Biophysical Chemistry 114 (2005) 103–113

Biophysical Chemistry

http://www.elsevier.com/locate/biophyschem

A theoretical study on the activation of Ser70 in the acylation mechanism of cephalosporin antibiotics

Yi-Yu Ke, Thy-Hou Lin*

Institute of Molecular Medicine and Department, of Life Science, National Tsing Hua University, Hsinchu, Taiwan 30043, Taiwan

Received 27 August 2004; received in revised form 15 November 2004; accepted 15 November 2004
Available online 30 November 2004

Abstract

A computational study using some molecular modeling and quantum mechanical methods has been performed for determining the most favor activation process for Ser70 in the acylation mechanism for the cephalosporin antibiotics among the three proposed ones given in the literature. The computation is based on an X-ray structure of the B chain of the *Bacillus licheniformis* BS3 β-lactamase–cefoxitin complex. The position of a catalytic water involved in one of the reaction mechanism is defined using the Grid20 and InsightII programs, while that of the truncated ligand is defined using the InsightII and FirstDiscovery programs. The geometry of structures of each reaction scheme is optimized at the HF/3-21 G level of theory, and then the single point energy for each reactive species in each reaction scheme is computed at the levels of HF/6−31+G (3df, 2p) and B3LYP/6−31+G (3df, 2p). The effect of solvent on each reaction scheme is also studied by comparing the calculation results for each reaction scheme either in gas phase or in solution using the HF/6−31+G (3df, 2p) level of theory. A computation using the B3LYP/6−31+G (3df, 2p) level of theory and the Polarized Continuum Model (PCM) and by treating water as a solvent is also conducted for each activation process. It is found that, energetically, the most favor activation process for Ser70 in the acylation mechanism is the one where a proton transfer is mediated by the catalytic water and the catalytic residues Glu166 and Ser70. This agrees with those observed in an ultrahigh resolution X-ray structure and a QM/MM theoretical study published recently on the same acylation process.

Keywords: Acylation mechanism; β-lactamase; Quantum mechanics; Proton transfer; Transition states; Reaction mechanism

1. Introduction

Cephalosporins is a class of β-lactam antibiotics where the β-lactam ring is fused to a six-membered dihydrothiazine ring rather than to the five-membered thiazolidine ring found in penicillins [1,2]. In the action against the Gram-negative bacteria, cephalosporins have a slight advantage over penicillins in passing through the porin channel because the cephalosporin nucleus is significantly less hydrophobic than the penicillin one [3]. Cephaloridine, especially, has a very high rate of diffusion through the outer membrane due to its zwitterionic nature [4]. However, to reach the targets that is the penicillin-binding proteins, these compounds have to overcome the periplasmic β-lactamases. These are the chromosomally coded enzymes present in most Gram-negative bacteria. They were previously called cephalosporinases because they were believed to hydrolyze cephalosporins much more effective than they do penicillins [5,6].

It is now known that class A β-lactamases are the predominate source of bacterial resistance to the β-lactam family of antibiotics, such as the penicillins and cephalosporins [7]. Therefore, these enzymes have been extensively studied for understanding the mechanistic nature of the resistance and for antiresistance drug design. The mechanism of proton abstraction and donation during hydrolysis of β-lactam antibiotics by the β-lactamases is still the subject of considerable

* Corresponding author. Tel.: +886 035742759; fax: +886 035715934.
E-mail address: thlin@life.nthu.edu.tw (T.-H. Lin).

0301-4622/$ - see front matter © 2004 Elsevier B.V. All rights reserved.
doi:10.1016/j.bpc.2004.11.007

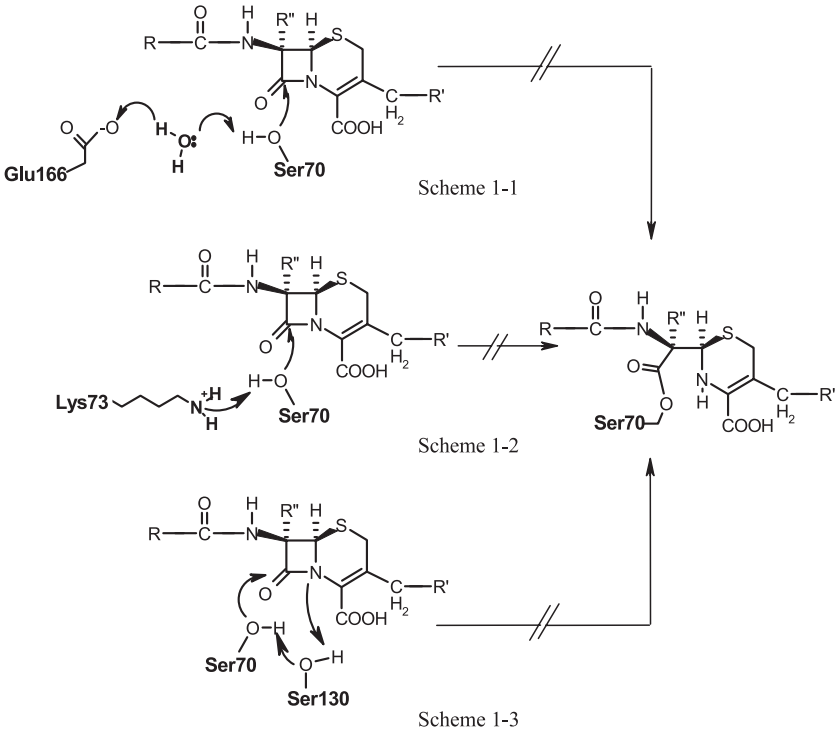

Scheme 1. (a) Scheme 1-1: Glu166 abstracts a proton from the γ-OH group of Ser70 via Wat1. (b) Scheme 1-2: The Nζ atom of Lys73 abstracts a proton from the γ-OH group of Ser70. (c) Scheme 1-3: A nucleophilic attack by Ser70 is accompanied by a simultaneous fission of the β-lactam ring and proton transfer to the leaving N atom which is assisted by the hydroxyl group of Ser130. The Oγ atom of Ser70 then attacks the carbonyl carbon atom of the β-lactam ring.

discussion. The active-site residues, which have been found to play an important catalytic role in the mechanism of all the class A β-lactamases, have been identified as follows: Ser70, Lys73, Lys234, Glu166, and Ser130 [8]. There are also three water molecules (Wat1, Wat2, and Wat3) being included in the active site [9–11]. Lamotte-Brasseur et al. [9] have proposed a catalytic mechanism in which the β-lactam ring is hydrolyzed by the class A enzyme through involvement of residues Ser70, Lys73, Ser130, Glu166, Wat1, and Wat2. As shown in Scheme 1-1, Glu166 abstracts the proton from the γ-OH group of Ser70 via Wat1. While losing its proton, the Oγ atom of Ser70 attacks the carbonyl carbon atom of the β-lactam ring. In the meantime, a proton is delivered back to the adjacent nitrogen atom via Wat2, Lys73, and Ser130, thus achieving the formation of the acyl-enzyme. Subsequently, Glu166 abstracts a proton from Wat1. By losing its proton, Wat1 attacks the carbonyl carbon atom of the Ser70 ester-linked acyl-enzyme. Then, reentry of a water replacing Wat1 allows Glu166 to deliver the proton back to the same carbonyl atom, thus achieving hydrolysis of the β-lactam ring and enzyme recovery.

There are ample site-directed mutagenesis and structural studies to show that Lys73 plays a key role in the catalytic process [12–17]. The deprotonated Lys73 can activate Ser70 for attacking on the lactam carbonyl carbon as shown in Scheme 1-2. The Nζ atom of Lys73 is found to be bound to the Oγ atom of Ser70 in several class A β-lactamase structures. The Lys73 residue is hypothesized as a catalytic base and must be deprotonated at physiological pH. However, some NMR studies suggest that the pK_a of the residue is greater than 10, which seem inconsistent with the hypothesis [18].

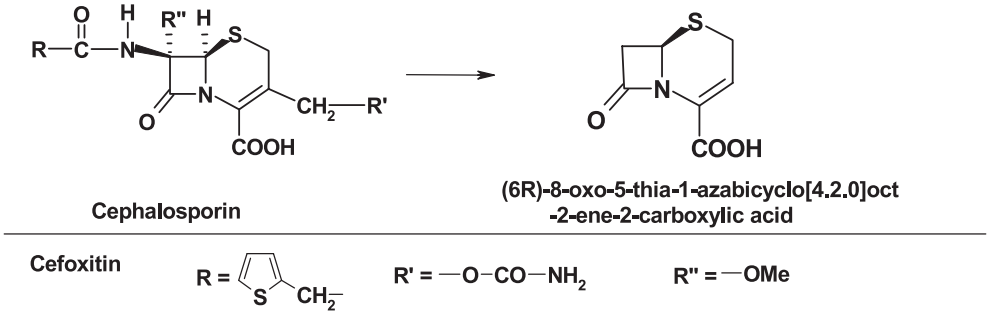

Scheme 2. The original and truncated forms of cephalosporin are shown in the left and right side, respectively.

Alternatively, others have assumed that the ϵ-amino group of Lys73, which is in close contact with Ser70 in the crystal structure, remains neutral due to the active site environment. The proton either directly from Ser70 or mediated by Wat1 can be transferred to the network of hydrogen bonds presumably formed by Lys73, Wat2, and the hydroxyl group of Ser130. A one-step mechanism for acylation involving the nucleophilic Ser70 and the hydroxyl group of Ser130 in class A enzymes has also been proposed [11]. As shown in Scheme 1-3, a nucleophilic attack by Ser70 causes simultaneous fission of the β-lactam ring and proton transfer to the leaving N atom which is assisted by the hydroxyl group of Ser130. This mechanism has been studied by several research groups [11,15,16]. In general, the acylation part of the reaction has remained controversial, although there is a consensus on the deacylation portion of the mechanism [17].

In this work, we have studied and compared the three activation processes in the acylation mechanism depicted in Schemes 1-1 to 1-3 for Ser70 using several molecular modeling and the ab initio quantum mechanical calculation methods. The structure of the *Bacillus licheniformis* BS3 β-lactamase–cefoxitin complex is used as the starting structure (ST). The catalytic water is carefully placed inside the active site of the enzyme using the program Grid20 [19] and the molecular dynamics simulation. The ligand cephalosporin is rigidly and then flexibly docked into the enzyme active size before being truncated as that shown in Scheme 2 for the ab initio quantum mechanical study. Our calculation indicates that Scheme 1-1 or that Glu166 acts through the catalytic water to activate Ser70 for nucleophilic attack on the β-lactam ring of the ligand is energetically the most favorable activation process for Ser70 in the acylation mechanism among the three, which is in accord with that observed in an ultrahigh resolution X-ray structure determined for a β-lactamase transition-state (TS) analogue complex [15] and a QM/MM

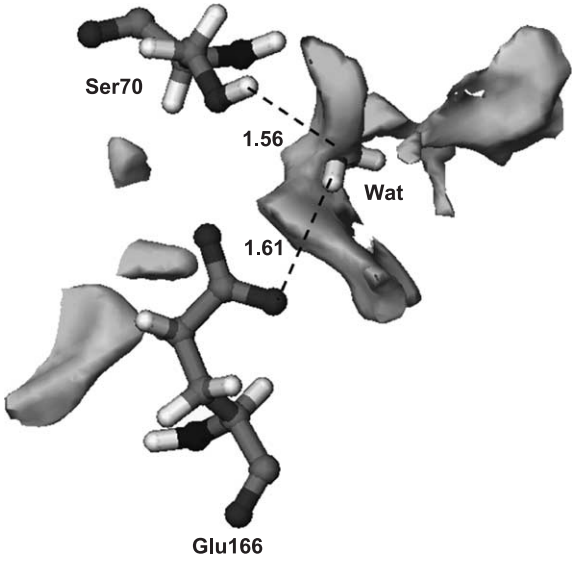

Fig. 1. Superposition of the catalytic water identified with the original meshwork generated by the Grid20 program [19].

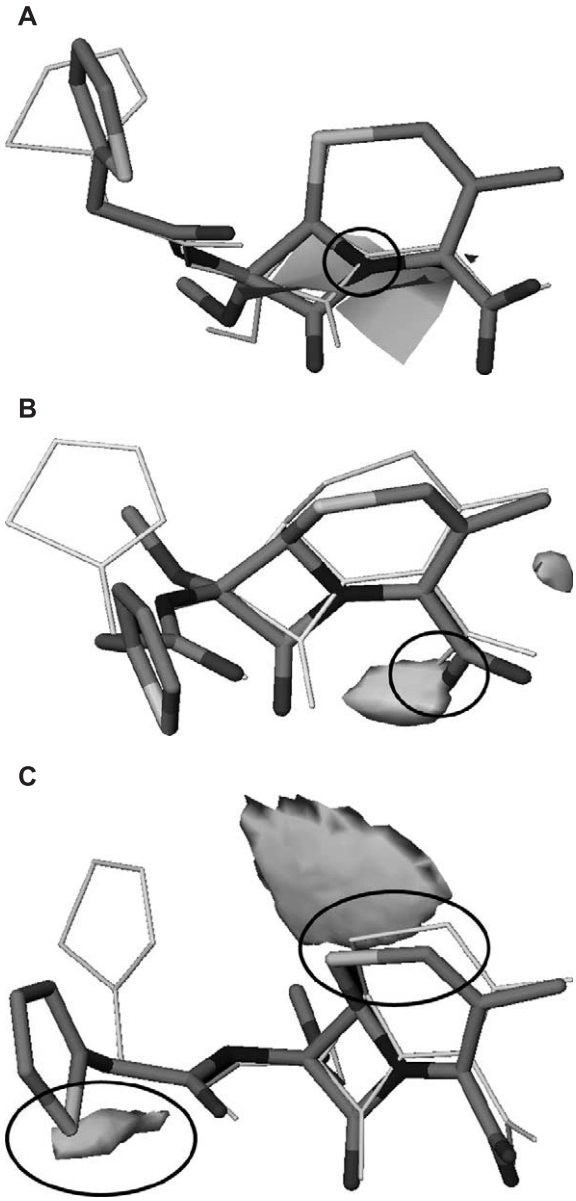

Fig. 2. (A) A comparison for the conformations of rigidly (represented with thin sticks) and flexibly (represented with thick sticks) docked cefoxitin in the active site of BS3 β-lactamase defined using the N1, COO^-, and Dry probes of the Grid20 program [19]. The superposition of N atom on the β-lactam ring with the N1 probe is highlighted with a circle. (B) A comparison for the conformations of rigidly (represented with thin sticks) and flexibly (represented with thick sticks) docked cefoxitin in the active site of BS3 β-lactamase defined using the N1, COO^-, and Dry probes of the Grid20 program [19]. The superposition of the carboxylic acid connected to the dihydrothiazine ring with the COO^- probe is highlighted with a circle. (C) A comparison for the conformations of rigidly (represented with thin sticks) and flexibly (represented with thick sticks) docked cefoxitin in the active site of BS3 β-lactamase defined using the N1, COO^-, and Dry probes of the Grid20 program [19]. The superposition of the carbon atoms on the dihydrothiazine ring with the Dry probe is highlighted with a circle.

Table 1
A comparison for distances determined between some selected atoms of the original and docked cefoxitin with those of some active site residues of the BS3 β-lactamase

	Protein atom	Distance (Å)	
		Original	Dock modify
β-lactam ring			
C4	Ser70.Oγ	1.5	2.6
	Ser70.N	3.2	5.1
	Ser130.Oγ	3.9	2.8
N1	Ser130.Oγ	3.2	2.5
Carboxylate			
O13	Ser130.Oγ	3.3	2.6
	Thr235.Oγ	3.2	2.5
O14	Gly236.N	3.3	4.2
	Arg244.Nη1	3.3	3.2
	Thr235.Oγ	2.6	3.2
R″			
O16	Lys73.Nζ	2.5	3.8
	Ser70.Oγ	2.3	2.4
	Ser130.Oγ	3.2	3.1
	Asn132.Oδ1	3.4	3.7

theoretical study published recently on the same acylation mechanism [17].

2. Materials and methods

The structure of the B chain of the *B. licheniformis* BS3 β-lactamase–cefoxitin complex taken from PDB (PDB entry 1I2W) was used as the starting structure [20]. There was no significant difference in coordinates of the backbone atoms of the two structures (A and B chains) given in the PDB file since the rms deviation computed was about 0.70. No crystal water was detected nearby the two important catalytic residues Glu166 and Ser70 when the structure of the ligand depleted enzyme was displayed using the RasMol program [21]. The favorite occupying positions for water molecules were predicted using the Grid20 program (Molecular Discov-

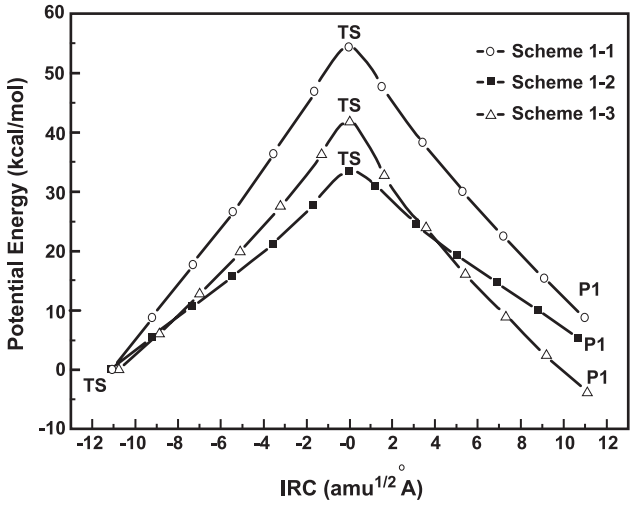

Fig. 4. The IRC calculation [26] results obtained for Scheme 1-1, 1-2, and 1-3. The abscissa represents the intrinsic reaction coordinate (IRC; amu$^{1/2}$ Å), and the ordinate represents the potential energy (kcal/mol).

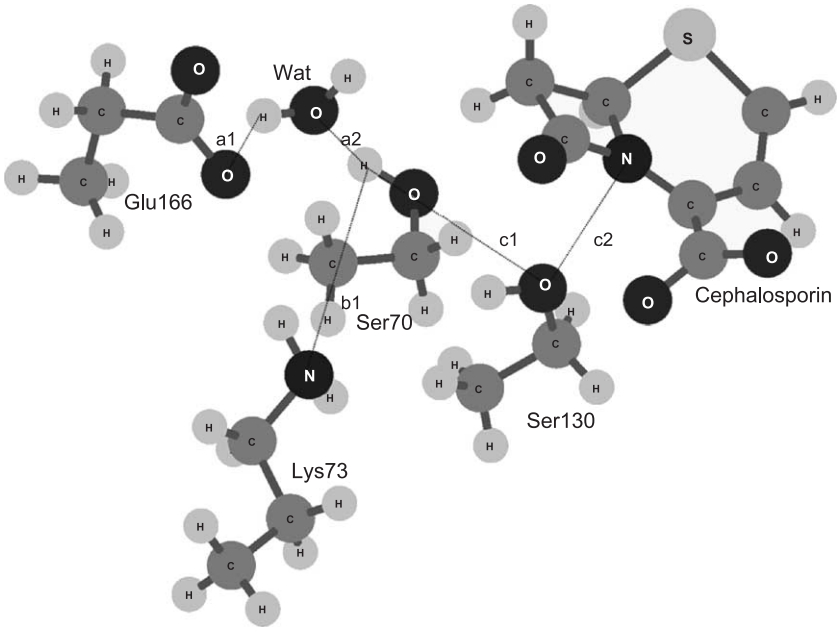

Fig. 3. The geometry of BS3 β-lactamase active site used for the identification of transition state structures for each activation scheme for Ser70 in the acylation mechanism. The catalytic water generated by the Grid20 program [19] and described in Fig. 1 is also included. Parameters used in Scheme 1-1 are a1 (distance between Oε1 of Glu166 and H of the catalytic water) and a2 (distance between O of the catalytic water and HOγ of Ser70), Scheme 1-2 is b1 (distance between HOγ of Ser70 and Nζ of Lys73), and Scheme 1-3 are c1 (distance between HOγ of Ser70 and Oγ of Ser130) and c2 (distance between HOγ of Ser130 and N1 of the β-lactam ring). Atoms that are fixed during the searching process in each activation scheme are marked with a start.

ery) [19]. First, a box of approximately 18 Å in dimension and centered at the ligand depleted active site where the catalytic residues Glu166 and Ser70 were included was constructed. The box was converted into a meshwork with a grid spacing of 0.25 Å. A water molecule was chosen as a probe to move on each grid point. The number of grid points or the number of water molecules that were able to form hydrogen bonds with the Oε or Oγ atom of Glu166 or Ser70 was identified to be 115. These water molecules were added into the active site of the enzyme where both the ligand and crystal waters were already depleted. A layer of waters of thickness 5 Å was added further to the active-site waters using the Soak module of the InsightII program (version 2000.0, Biosym Technologies) [22]. The water-added enzyme was solvated in a layer of waters of thickness 10 Å. The whole system was shortly minimized by 500 steps of Steepest Descent method [22] before being subjected to 3000 steps of molecular dynamics simulation using the InsightII program and the cff91 force field [22]. The most proximate water molecule to both the Oε and Oγ atoms of Glu166 and Ser70 was identified and isolated as the catalytic water after the molecular dynamics simulation runs.

The β-lactam ring of ligand cefoxitin separated from the enzyme was an opened form. The β-lactam ring was restored in the closed form, and the entire ligand was briefly energy minimized using the SYBYL 6.8 program (Tripos) [23], and the Gasteiger-Hückel charges[24] were added. The energy-minimized ligand was docked into the enzyme active site filled with the catalytic water using the AutoGroup module of the Grid20 program [19]. This was a rigid docking process for which a box of 18 Å in dimension was constructed over the active site where the following catalytic residues Glu166, Ser70, Ser130, Lys73, and Lys234 were included. The exact position for docking the ligand into the active site was defined using some Grid20 [19] probes such as N1, COO^-, and Dry for representing the favorite positions for the N, carboxyl, and hydrophobic groups, respectively. A flexible docking was subsequently performed for the best five docked conformations obtained from the rigid docking using the Glide module of the FirstDiscovery program (Schrödinger) [25]. The flexibly docked conformations were compared with the molecular fields generated in the active site of the enzyme by the Grid20 program [19] using the N1, COO^-, and Dry probes. The conformation that was best matched with all the molecular fields generated in the active site of the enzyme was selected as the starting geometry for the quantum mechanics calculation. However, all the R, R', and R" groups on the original structure were truncated (Scheme 2) for proceeding with the quantum mechanics calculation.

The ab initio and Density Functional Theory (DFT) quantum mechanical calculations were conducted using the Gaussian 98 program [26] for all the reaction paths depicted in Schemes 1-1 to 1-3. To proceed with the quantum mechanical calculations, the active site residues critically involved in the reactions, namely, Glu166, Ser70, and Lys73, were truncated respectively into the following

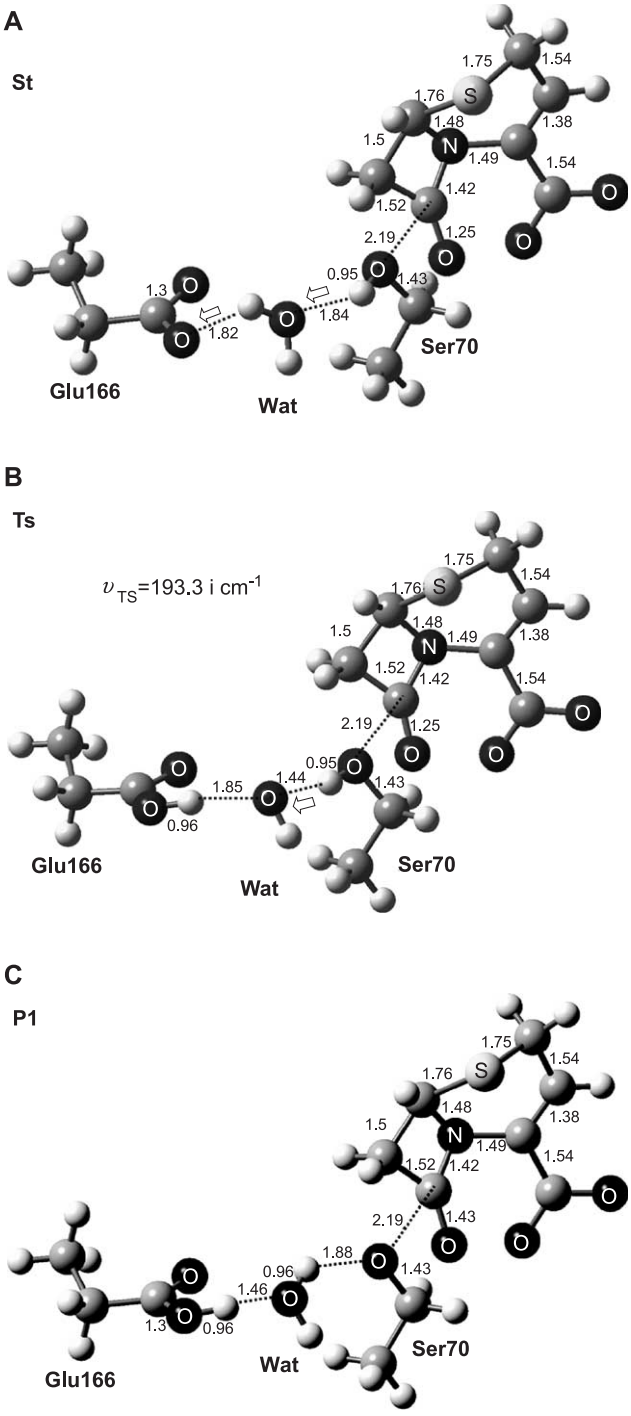

Fig. 5. (A) The geometry of the starting structures of the activation Scheme 1-1. The distances between pairs of atoms determined are in angstroms. The direction of proton transfer is marked with an arrow. (B) The geometry of the transition state searched for the activation Scheme 1-1. The imaginary frequency computed is also shown. The distances between pairs of atoms determined are in angstroms. The direction of proton transfer is marked with an arrow. (C) The geometry of the reaction product of the activation Scheme 1-1. The distances between pairs of atoms determined are in angstroms.

groups: $CH_3CH_2COO^-$, CH_3CH_2OH, and $CH_3CH_2CH_2NH_2$. The geometry of all the starting structures was optimized using the Steepest Descent method of the InsightII program [22]. The atomic coordinates of truncated cephalosporin in each activation process were fixed during the optimization process. The transition-state structure for each reaction path was determined by a vibrational analysis to search the mode with an imaginary frequency computed as described by Tsuda et al. [27] and Hata et al. [28]. There were 18, 9, and 11 imaginary frequencies computed for each starting structure in Schemes 1-1 to 1-3, respectively. To search the transition-state structure, the vibrational mode which best correlates with the direction of proton donation and abstraction was identified for each scheme. The steepest descent paths from the transition state were calculated in both directions following the vibrational mode, which provided the lowest energy reaction path connecting a reactant and a product (P1) via the saddle point. These were the intrinsic reaction coordinate (IRC) [26,29] calculations which generated both the structural and potential energy changes along the reaction path searched. The single point energies along each reaction path were computed using the HF/6−31+G (3df, 2p) and B3LYP/6−31+G (3df, 2p) levels of theories. The solvation effect on each reaction was also accounted by using the Polarized Continuum Model (PCM) [26,30] and treating water as the solvent.

3. Results and discussion

The BS3 β-lactamase is composed of two globular domains, and the catalytic pocket is located at the interface between the two domains. The center of active site is occupied by residues Ser70, Thr71, Ile72, Lys73, Ser130, Asp131, and Asn132, while residues Glu166 and Asn170 are pointed to the cavity from the bottom [20]. There are also two crystal waters, namely, Wat302 and Wat303, detected in the active site of the enzyme. Wat302 appears to interact with residues Ser70 and Glu166, while Wat303 interacts with the oxyanion hole formed by the NH groups of residues Ala237 and Ser70 and also with an oxygen atom of a carboxylate group of the citrate ion. However, these two crystal waters are too distal to the Oγ or Oϵ atoms of Ser70 or Glu166 when the structure is displayed using the RasMol program [21]. In fact, the nearest water to the above two catalytic groups identified by the RasMol program [21] is Wat310 and which is 6.44 or 7.16 Å away from the two groups. To define the location of the catalytic water, we use the Grid20 program [19] to find a box of waters inside the enzyme active site and around the two important catalytic residues Ser70 and Glu166. The positions of these waters are fine-tuned through a docking process and brief molecular dynamics simulation runs using the InsightII program [22]. There are 115 waters being found inside the enzyme active site after the treatment of docking and solvation processes. As shown in Fig. 1, the most proximate water to the two important catalytic groups is identified as the catalytic water in which the corresponding distances determined between them are 1.56 and 1.66 Å, respectively. The position of the catalytic water identified is also superimposable with the original meshwork where the water is created by the Grid20 program [19] (Fig. 1).

To place the separated and truncated cefoxitin ligand (Scheme 2) back into the active site, a combination of rigid and flexible docking processes is conducted for the ligand. The primary cavity for rigid docking is defined using the N1, COO^-, and Dry probes of the Grid20 program [19]. The flexible docking is subsequently performed to fine-tune the conformation of the docked ligand. The conformations of rigid and flexible docked ligand are compared in Fig. 2A–C along with the highlighted positions of the catalytic cavity defined by the N1, COO^-, and Dry probes of the Grid20 program [19]. Apparently, the conformations of the two docked structures are very similar except that of the 2-methythiophene ring (Fig 2A–C). The positions of N atom on the lactam ring (N1), the carboxylic acid connected to the dihydrothiazine ring (COO^-), and the carbon atoms on the dihydrothiazine ring (hydrodrophobic) of the two docked conformations are all matched with those defined with the three probes of the Grid20 program [19] (Fig. 2A–B). A comparison for atomic distances between atoms of some active site residues and those of the original and docked ligands are given in Table 1. The overall position of the docked ligand is slightly deviated from that of the original one since there is a slight difference in position of the lactam ring (distances between C4 or N1 atoms of the ring and N or Oγ atoms of the active site residues Ser70 or Ser130 are slightly different) and that of the carboxyl

Table 2
Mulliken charges computed for atoms on the catalytic residues involved in each activation process for Ser70 in the acylation mechanism

Atom involved in each reaction scheme	Scheme 1-1			Scheme 1-2			Scheme 1-3		
	ST	TS	P1	ST	TS	P1	ST	TS	P1
β-lactam ring C4	1.52	1.48	1.43	1.46	1.39	1.39	1.54	1.55	1.51
β-lactam ring N1	–	–	–	–	–	–	−0.52	0.10	0.09
Cata water O	0.01	−0.74	−0.04	–	–	–	–	–	–
Glu 166 Oε1	−0.97	−0.22	−0.18	–	–	–	–	–	–
Lys 73 Nζ	–	–	–	0.14	0.47	0.59	–	–	–
Ser 70 Oγ	−0.22	−0.23	−0.70	−0.51	−0.62	−0.69	−0.34	−0.49	−0.45
Ser130 Oγ	–	–	–	–	–	–	−0.52	−0.46	−0.57

group connected to the ring (distances between O13 or O14 atoms of the connected carboxyl group and Oγ atoms of the active site residues Ser130 and Thr235 or N atom of Gly236 are also slightly different) (Table 1). The docked ligand is truncated by removing the three major side chains, namely, R, R', and R", to proceed with the quantum mechanic calculation (Scheme 2).

To search the transition state, we adopt the procedures previously described by Tsuda et al. [27] and Hata et al. [28]. First, an atomic geometry of the transition state is roughly determined by using some distances defined in each reaction scheme shown in Fig. 3 as parameters. A geometry optimization is performed for each reaction scheme while keeping each distance fixed. The calculations are repeated while changing only one of the two parameters by increments of 0.1–0.5 Å. The structure of the transition state in each reaction scheme is deduced by examining the potential energy change obtained by the above trials. Then, a geometry optimization is performed again for the deduced structure using the transition state search algorithm [26]. An IRC analysis [26] is conducted further to confirm that the optimized structure is appropriate for the saddle point. As shown in Fig. 4, the reaction path for each reaction scheme is determined through the IRC [26] calculations by starting from each transition-state structure searched. The abscissa represents the IRC distance measured from the transition state, while the ordinate indicates the potential energy computed (Fig. 4). The corresponding geometries of the starting structure (ST), transition state (TS), and product (P1) for Schemes 1-1 to 1-3 are presented in Figs. 5A–C, 6A–C, and 7A–C, respectively.

The distance between the β-lactam carbonyl carbon atom C4 and the Oγ atom of Ser70 shown in Fig. 5A is 2.19 Å, which agrees well with that given by Lamotte-Brasseur et al. [9] for the same reaction pathway for cephalosporin C. A hydrogen bond network may form between the proton of the catalytic water and Oε1 atom of Glu166 and also between the O atom of the catalytic water and that of Ser70 since the distances between them are 1.82 and 1.84 Å, respectively (Fig. 5A). The vibrational mode with an imaginary frequency computed is defined as the directions of the proton donation or abstraction as highlighted in Fig. 5A. For the TS identified, the proton of the catalytic water is transferred to the Oε1 atom of Glu166 to form a new chemical bond, while that of Ser70 is being abstracted by the O atom of the catalytic water (Fig. 5B). The corresponding imaginary frequency computed is 193.3 i cm^{-1}. The reaction product is depicted in

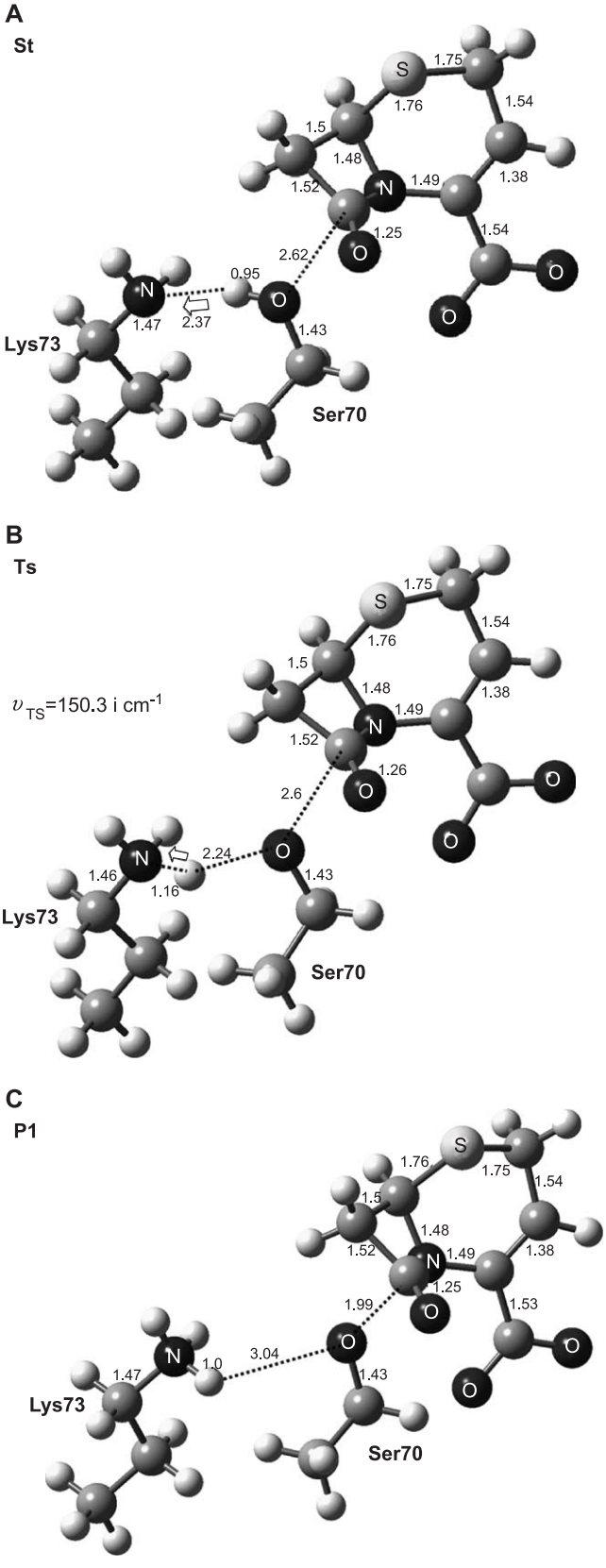

Fig. 6. (A) The geometry of the starting structures of the activation Scheme 1-2. The distances between pairs of atoms determined are in angstroms. The direction of proton transfer is marked with an arrow. (B) The geometry of the transition state searched for the activation Scheme 1-2. The imaginary frequency computed is also shown. The distances between pairs of atoms determined are in angstroms. The direction of proton transfer is marked with an arrow. (C) The geometry of the reaction product of the activation Scheme 1-2. The distances between pairs of atoms determined are in angstroms.

Fig. 5C, where the catalytic water is protonated and the Oγ atom of deprotonated Ser70 is bridging with the carbonyl carbon atom C4 of β-lactam ring with a distance of 2.19 Å. The progress of proton donation and abstraction in the activation process is also revealed by the change of Mulliken charges computed for each atomic species involved, as shown in Table 2. While there is no significant change in the Mulliken charge on the C4 atom of β-lactam ring computed on going from the ST, TS, to P1 state, an obvious change in the charge of the Oε1 atom of Glu166 on going from the ST to TS (abstraction of a proton from the catalytic water) or that for the Oγ atom of Ser70 on going from the TS to P1 (donation of a proton to the catalytic water) state is observed (Table 2).

Instead of losing a proton to the catalytic water, the proton of Ser70 is transferred to the Nζ atom of Lys73 in Scheme 1-2 (Fig. 6A). The Nζ atom of Lys73 in the scheme is treated as deprotonated and neutral in the ST structure (Fig. 6A). A TS of an imaginary frequency 150.3 i cm^{-1} is searched for the reaction pathway (Fig. 6B). The corresponding reaction product is depicted in Fig. 6C where the Nζ atom of Lys73 is now protonated. The Mulliken charge on the protonated Nζ atom of Lys73 in the P1 state is more positive than that in the TS (Table 2), indicating that the proton donated by Ser70 is nearly bound to the Nζ atom of Lys73. Note that the distance between the Oγ atom of Ser70 and the C4 atom of β-lactam ring is also apparently shortened from the TS to P1 state (Fig. 6B and C).

A tetrahedral species is formed in Scheme 1-3 where the deprotonated Oγ atom of Ser70 is attacking the C4 atom of β-lactam ring, and the N atom on the same ring is abstracting a proton from the Oγ atom of Ser130 (Fig. 7A). A transition state with an imaginary frequency of 393.3 i cm^{-1} is searched, where the Oγ atom of Ser130 is gaining a proton from the Oγ atom of Ser70 and losing its proton to the N atom of β-lactam ring (Fig. 7B). However, in the P1 state shown in Fig. 7C, the abstraction of proton by the latter appears to be incomplete since the distance between them is 1.18 Å, and that between the attacking Oγ atom of Ser70 and the C4 atom of β-lactam ring is 2.56 Å, which is unchanged from that observed in the TS (Fig. 7B). There is a change in the Mulliken charge computed for the Oγ atom of Ser70 on going from the ST to TS, but no significant change is observed in the charge computed for the Oγ atom of Ser130 (Table 2). Moreover, while the Mulliken charge computed for the N1 atom of β-lactam ring is changing from −0.52 in state ST to 0.09 in state P1, that computed for the C4 atom on the same ring in each same state is not significantly changed as that observed for the other two schemes (Table 2).

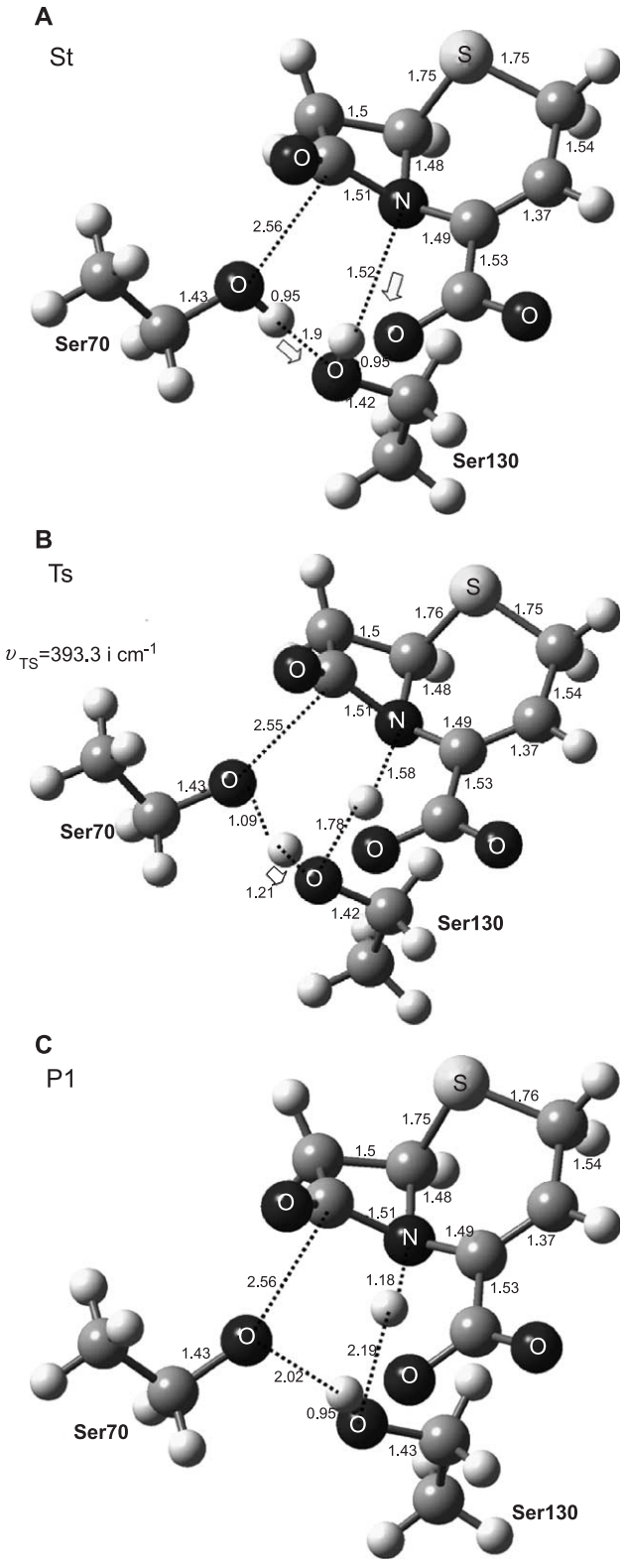

Fig. 7. (A) The geometry of the starting structures of the activation Scheme 1-3. The distances between pairs of atoms determined are in angstroms. The direction of proton transfer is marked with an arrow. (B) The geometry of the transition state searched for the activation Scheme 1-3. The imaginary frequency computed is also shown. The distances between pairs of atoms determined are in angstroms. (C) The geometry of the reaction product of the activation Scheme 1-3. The distances between pairs of atoms determined are in angstroms.

A gas phase computation at the HF/6−31+G (3df, 2p) level of theory for each reaction scheme has also been performed to assess the effect of solvent on each reaction scheme. The dipole moment of each reaction scheme in gas phase or in solution is also computed and compared as shown in Table 3. An obvious change in the dipole moment computed for Scheme 1-1 can be seen when it is shifted from gas phase to solution. However, there is only a slight change in dipole moment computed for Schemes 1-2 and 1-3 when they are shifted from gas phase to solution. The effect of solvent on both the TS and P1 states of Scheme 1-1 computed by the HF/6−31+G (3df, 2p) level of theory is much stronger than that computed on the same states of the other two schemes. The corresponding energy computed for each state of each reaction scheme listed in Table 4 shows that both the TS and P1 states of Scheme 1-1 are more stabilized by the solvent than those of the other two schemes. The greater dipole moments computed for the structures in the TS or P1 state in Scheme 1-1 means that the polarity of these structures are greater, thereby the polarization of the solvent continuum is greatly enhanced. On the other hand, the smaller dipole moments computed for structures in Schemes 1-2 and 1-3 indicate that charges on them are more delocalized, thus causing the polarization of the solvent continuum to decrease.

The single point energies computed using either the HF/6−31+G (3df, 2p) or B3LYP/6−31+G (3df, 2p) level of theories for states in Scheme 1-2 and 1-3 are all larger than those computed for states in Scheme 1-1 (Table 4). In fact, the single point energies computed in gas phase using the HF/6−31+G (3df, 2p) level of theory for states in Scheme 1-1 are also smaller than those computed for states in both Schemes 1-2 and 1-3 (Table 4). The single point energy computed using the B3LYP/6−31+G (3df, 2p) level of theory for each state in each scheme is also smaller than that computed using the HF/6−31+G (3df, 2p) level of theory. However, the order of energy barrier of each scheme computed by the HF/6−31+G (3df, 2p) level of theory is similar to that by the B3LYP/6−31+G (3df, 2p) one, as presented in Table 4. The order of energy barrier of each reaction scheme computed by both theoretical methods is Scheme 1-3>1-2>1-1 (Table 4), indicating that Scheme 1-1 is the most favorable activation process for Ser70 in the acylation mechanism among all the three pathways studied.

The fact that Glu166 is more likely to be a proton abstractor than Lys73 has also been addressed by others [31–33] using the pK_a values computed for the two catalytic residues. These are in parallel with the result presented here. Recent ultrahigh resolution X-ray structure determined by Minasov et al. [15] for TEM-1 β-lactamase has revealed that a proton is indeed being shuttled from Ser70 through a catalytic water to end up on Glu166. It is also observed that Lys73 forms hydrogen bonds with both Ser70 and Ser130, which may activate both residues electrostatically [15]. Lys73 may also act to transfer a proton to replace the one Ser130 has donated in activating the lactam nitrogen. Such a proton transfer might be essential for an efficient deprotonation of Glu166 for deacylation process. In fact, a recent NMR pK_a measurement for Lys73 also indicates that Glu166 is the most likely candidate as a general base role in the acylation mechanism by acting through a catalytic water [18].

Table 3
Dipole moments computed for each reaction species in each reaction scheme in gas phase or in solution at the HF/6−31+G (3df, 2p) level of theory

	μ (Gas phase)	μ (Solution)
Scheme 1-1		
ST	23.2D[a]	36.5D
TS	19.0D	29.5D
P1	9.1D	13.7D
Scheme 1-2		
ST	6.7D	9.8D
TS	16.1D	19.6D
P1	30.7D	35.2D
Scheme 1-3		
ST	6.0D	9.9D
TS	12.0D	16.8D
P1	13.6D	19.6D

[a] The unit of dipolemoment computed is in Debye (D).

Table 4
The single point energy computed for each reaction species in each reaction scheme

	HF6−31G +(3df, 2p) (hartree)	E (kcal/mole)	B3LYP 6−31G+(3df, 2p) (hartree)	E (kcal/mole)
Scheme 1-1				
ST	−1440.9523 (−1440.8463)	–	−1447.8793	–
TS	−1440.9412 (−1440.7919)	6.97 (34.13)	−1447.874956	2.73
P1	−1441.0159 (−1440.9226)	−39.91 (−47.87)	−1447.9280	−30.56
Scheme 1-2				
ST	−1272.5228 (−1272.4823)	–	−1278.5162	–
TS	−1272.4418 (−1272.3589)	50.83 (77.43)	−1278.4550	38.40
P1	−1272.4832 (−1272.3331)	24.85 (93.62)	−1278.5263	−6.34
Scheme 1-3				
ST	−1253.2968 (−1253.2642)	–	−1259.0437	–
TS	−1253.0797 (−1253.0281)	136.23 (148.155)	−1258.9294	71.72
P1	−1253.2454 (−1253.1623)	32.25 (63.94)	−1259.0030	25.54

The single point energy computed for each reaction species of each reaction scheme in gas phase is in parenthesis.

4. Conclusion

Three activation processes for Ser70 in the acylation mechanism for hydrolysis of cephalosporin antibiotics catalyzed by a class A β-lactamase are studied and compared using the molecular modeling and quantum mechanics approaches. The position of a catalytic water participating in the most favorable activation process identified for Ser70 involving both Glu166 and Ser70 catalytic residues is defined by using the molecular modeling technique. The importance of correctly placing the catalytic water into the active site has been demonstrated by a site-directed mutagenesis study on the hydrolysis of benzylpenicillin by the E166D or K73R mutant of *Bacillus cereus* β-lactamase [34]. The rate constant measured for the former is about 20-fold less than that for the latter due to the fact that the catalytic water in the former is unable to connect the hydroxyl group of Ser70 to the dicarboxylic acid, thereby the proton abstraction process is severely hampered [33]. Our calculation excludes the possible involvement by Lys73 treated as neutral form in the activation process for Ser70 in the acylation mechanism, which is in accord with a recent QM/MM theoretical study on the same mechanism in which Lys73 is treated as protonated form [17]. We have also shown here that Ser70 is unlikely to be activated in the acylation mechanism by a concerted reaction involving both N1 and C4 atoms of the β-lactam ring and the hydroxyl group of Ser130.

The dipole moments and single point energy for each reaction species in gas phase or in solution are also computed and compared to examine the effect of solvation on the progress of each activation process for Ser70 in the acylation mechanism. By including the solvent continuum, it is found that the energy barrier computed using higher level of density functional theory for each activation process is much lowered than that computed using the Hartree-Fock-based method. As expected, the solvent continuum has the largest effect on the transition state where charge separation is most significant. Since the active site of the enzyme is not only exposed to solvent but also surrounded by a large amount of protein framework, it is also necessary to consider the effect of protein environment on the activation processes. However, it is difficult to model the solvent–protein mixed environment computationally. One may handle the two different environments individually by treating the protein component through specific directional potentials while the bulk solvent through some type of solvent continuum. The effect of protein environment on a reaction mechanism similar to Scheme 1-3 studied here has been presented by Díaz et al. [11] using the Divide and Conquer (D&C) linear scaling approach. They found that all the transition states searched are stabilized by about 5 kcal/mol by including the effect of protein environment. However, there are still undetermined parameters such as the entropic contributions arising from the structural elasticity of the protein environment in such an approach. Therefore, more detailed models using quantum and molecular mechanical techniques are required to further explore the role of each molecular species participating in each activation process for Ser70 in the acylation mechanism.

Acknowledgement

This work is supported in part by a grant (NSC92-2313-B007-002) from the National Science Council, Taiwan. All the molecular modeling and quantum mechanical calculations described in this work are conducted at the National Center for High-Performance Computing, Taiwan.

References

[1] S. Kovacevic, B.J. Weigel, M.B. Tobin, T.D. Ingolia, J.R. Miller, Cloning, characterization, and expression in *Escherichia coli* of the streptomyces clavuligerus gene encoding deacetoxycephalosporin C synthetase, J. Bacteriol. 171 (1989) 754–760.
[2] J.L. Barredo, J.F. Martin, Genes directly involved in the biosynthesis of beta-lactam antibiotics, Microbiologia 7 (1991) 1–12.
[3] T. Hashizume, M. Sanada, S. Nakagawa, N. Tanaka, Alteration in expression of *Serratia marcescens* porins associated with decreased outer membrane permeability, J. Antimicrob. Chemother. 31 (1993) 21–28.
[4] J. Mitsuyama, R. Hiruma, A. Yamaguchi, T. Sawai, Identification of porins in outer membrane of *Proteus*, *Morganella*, and *Providencia* spp. and their role in outer membrane permeation of beta-lactams, Antimicrob. Agents Chemother. 31 (1987) 379–384.
[5] F.P. Tally, G.J. Cuchural Jr., M.H. Malamy, Mechanisms of resistance and resistance transfer in anaerobic bacteria: factors influencing antimicrobial therapy, Rev. Infect. Dis. 1 (1984) 260–269.
[6] H.C. Neu, Contribution of beta-lactamases to bacterial resistance and mechanisms to inhibit beta-lactamases, Am. J. Med. 79 (1985) 2–12.
[7] J.T. Smith, J.M. Hamilton-Miller, R. Knox, Bacterial resistance to penicillins and cephalosporins, J. Pharm. Pharmacol. 21 (1969) 337–358.
[8] R.P. Ambler, A.F. Coulson, J.M. Frére, J.M. Ghuysen, B. Jaurin, B. Joris, R. Levesque, G. Tiraby, S.G. Waley, A standard numbering scheme for the class A beta-lactamases, Biochem. J. 276 (1991) 269–270.
[9] J. Lamotte-Brasseur, G. Dive, O. Dideberg, P. Charlier, J.M. Frére, J.M. Ghuysen, Mechanism of acyl transfer by the class A serine β-lactamase of *Streptomyces albus* G, Biochem. J. 279 (1991) 213.
[10] S. Wolfe, C.-K. Kim, K. Yang, Ab initio molecular orbital calculation on the neutral and methanolysis of azetidinones, including catalysis water, relationship to the mechanism of action of β-lactam antibiotics, Can. J. Chem. 72 (1994) 1014–1032.
[11] N. Diaz, D. Suarez, T.L. Sordo, K.M. Merz Jr., Acylation of Class A beta-lactamase by penicillins: a theoretical examination of the role of serine 130 and the -lactam carboxylate group, J. Phys. Chem., B 105 (2001) 11302–11313.
[12] N.C. Strynadka, R. Martin, S.E. Jensen, M. Gold, J.B. Jones, Structure-based design of a potent transition state analogue for TEM-1 beta-lactamase, Nat. Struct. Biol. 3 (1996) 688–695.
[13] N.C. Strynadka, H. Adachi, S.E. Jensen, K. Johns, A. Sielecki, C. Betzel, K. Sutoh, M.N. James, Molecular structure of the acyl-enzyme intermediate in beta-lactam hydrolysis at 1.7 A resolution, Nature 359 (1992) 700–705.

[14] Y.C. Leung, C.V. Robinson, R.T. Aplin, S.G. Waley, Site-directed mutagenesis of beta-lactamase I: role of Glu-166, Biochem. J. 229 (1994) 671–678.
[15] G. Minasov, X. Wang, B.K. Shoichet, An ultrahigh resolution structure of TEM-1 -lactamase suggests a role for Glu166 as the general base in acylation, J. Am. Chem. Soc. 124 (2002) 5333.
[16] J. Pitarch, J-.L. Pascual-Ahuir, E. Silla, I. Tuñón, A quantum mechanics/molecular mechanism study of the acylation reaction of TEM1 β-lactamase and penicillance, J. Chem. Soc., Perkin Trans. 2 (2000) 761–767.
[17] J.C. Hermann, L. Ridder, A.J. Mulholland, H.-D. Holtje, Identification of Glu166 as the general base in the acylation reaction of class A -lactamases through QM/MM modeling, J. Am. Chem. Soc. 125 (2003) 9590–9591.
[18] C. Damblon, X. Raquet, L.Y. Lian, J. Lamotte-Brasseur, E. Fonze, P. Charlier, G.C. Roberts, J.M. Frere, The catalytic mechanism of beta-lactamases: NMR titration of an active-site lysine residue of the TEM-1 enzyme, Proc. Natl. Acad. Sci. U. S. A. 93 (1996) 1747–1752.
[19] P.J. GoodFord, A computational procedure for determining energetically favorable binding sites on biologically important macromolecules, J. Med. Chem. 28 (1985) 849–857.
[20] E. Fonzé, M. Vanhove, G. Dive, E. Sauvage, J.M. Frère, P. Charlier, Crystal structures of the *Bacillus licheniformis* BS3 class A -lactamase and of the acyl-enzyme adduct formed with cefoxitin, Biochemistry 41 (2002) 1877–1885.
[21] R.A. Sayle, E.J. Milner-Whilte, RASMOL: biomolecular graphics for all, Trends Biochem. Sci. 20 (1995) 374–382.
[22] Insight II Program, Biosym/MSI, San Diego, CA, (1995).
[23] Sybyl, version 6.8, Tripos: St. Louis, MO.
[24] J. Gasteiger, M. Marsili, Iterative partial equalization of orbital electronegativity—a rapid access to atomic charges, Tetrahedron 36 (1980) 3219–3228.
[25] T.A. Halgren, R.B. Murphy, R.A. Friesner, H.S. Beard, L.L. Frye, W.T. Pollard, J.L. Banks, Glide: a new approach for rapid, accurate docking and scoring: 2. Enrichment factors in database screening, J. Med. Chem. (2004) (ASAP Article).
[26] Gaussian 98., Revision A.6., M.J. Frisch, G.W. Trucks, H.B. Schlegel, G.E. Scuseria, M.A. Robb, J.R. Cheeseman, V.G. Zakrzewski, J.A. Montgomery, R.E. Stratmann Jr., J.C. Burant, S. Dapprich, J.M. Millam, A.D. Daniels, K.N. Kudin, M.C. Strain, O. Farkas, J. Tomasi, V. Barone, M. Cossi, R. Cammi, B. Mennucci, C. Pomelli, C. Adamo, S. Clifford, J. Ochterski, G.A. Petersson, P.Y. Ayala, Q. Cui, K. Morokuma, D.K. Malick, A.D. Rabuck, K. Raghavachari, J.B. Foresman, J. Cioslowski, J.V. Ortiz, B.B. Stefanov, G. Liu, A. Liashenko, P. Piskorz, I. Komaromi, R. Gomperts, R.L. Martin, D.J. Fox, T. Keith, M.A. Al-Laham, C.Y. Peng, A. Nanayakkara, C. Gonzalez, M. Challacombe, P.M.W. Gill, B. Johnson, W. Chen, M.W. Wong, J.L. Andres, C. Gonzalez, M. Head-Gordon, E.S. Replogle, J.A. Pople, Gaussian, Pittsburgh, PA, 1998.
[27] N. Tsuda, M. Hata, T. Hoshino, M. Tsuda, Ab initio study of the role of lysine 16 for the molecular switching mechanism of Ras protein p21, Biophys. J. 32 (1999) 3287–3292.
[28] M. Hata, Y. Fujii, M. Ishii, T. Hoshino, M. Tsuda, Catalytic mechanism of class A beta-lactamase: I. The role of Glu166 and Serl30 in the deacylation reaction, Chem. Pharm. Bull. (Tokyo) 48 (2000) 447–453.
[29] C. Gonzalez, H.B. Schlegel, An improved algorithm for reaction path following, J. Chem. Phys. 90 (1989) 2154.
[30] S. Miertus, J. Tomasi, Approximate evaluations of the electrostatic free energy and internal energy changes in solution processes, Chem. Phys. 65 (1982) 239–245.
[31] X. Raquet, V. Lounnas, J. Lamotte-Brasseur, J.M. Frere, R.C. Wade, pK_a calculations for Class A β-lactamase: methodological and mechanistic implications, J. Biophys. 73 (1997) 2416–2426.
[32] J. Lamotte-Brasseur, V. Lounnas, X. Raquet, R.C. Wade, pK_a calculation for class A β-lactamase: influence of substrate binding, Protein Sci. 8 (1999) 404–409.
[33] I. Massova, P.A. Kollman, pK_a, MM, and QM studies of mechanisms of beta-lactamases and penicillin-binding proteins: acylation step, J. Comput. Chem. 23 (2002) 1559–1576.
[34] R.M. Gibson, H. Christensen, S.G. Waley, Site-directed mutagenesis of beta-lactamase I single and double mutants of Glu-166 and Lys-73, Biochem. J. 272 (1990) 613–619.